Journal of Marine Systems 181 (2018) 25–36

Contents lists available at ScienceDirect

Journal of Marine Systems

journal homepage: www.elsevier.com/locate/jmarsys

An analysis on half century morphological changes in the Changjiang Estuary: Spatial variability under natural processes and human intervention

Jie Zhao[a], Leicheng Guo[a,*], Qing He[a], Zheng Bing Wang[a,b,c], D.S. van Maren[b,c], Xianye Wang[a]

[a] State Key Laboratory of Estuarine and Coastal Research, East China Normal University, Shanghai 200062, People's Republic of China
[b] Faculty of Civil Engineering and Geosciences, Delft University of Technology, P.O. Box 5048, NL-2600, GA, Delft, The Netherlands
[c] Deltares, WL | Delft Hydraulic, P.O.Box 177, NL-2600, MH, Delft, The Netherlands

ARTICLE INFO

Keywords:
Changjiang Estuary
Morphological evolution
Sediment supply

ABSTRACT

Examination of large scale, alluvial estuarine morphology and associated time evolution is of particular importance regarding management of channel navigability, ecosystem, etc. In this work, we analyze morphological evolution and changes of the channel-shoal system in the Changjiang Estuary, a river- and tide-controlled coastal plain estuary, based on bathymetric data between 1958 and 2016. We see that its channel-shoal pattern is featured by meandering and bifurcated channels persisting over decades. In the vertical direction, hypsometry curves show that the sand bars and shoals are continuously accreted while the deep channels are eroded, leading to narrower and deeper estuarine channels. Intensive human activities in terms of reclamation, embankment, and dredging play a profound role in controlling the decadal morphological evolution by stabilizing coastlines and narrowing channels. Even though, the present Changjiang Estuary is still a pretty wide and shallow system with channel width-to-depth ratios > 1000, much larger than usual fluvial rivers and small estuaries. In-depth analysis suggests that the Changjiang Estuary as a whole exhibited an overall deposition trend over 59 years, i.e., a net deposition volume of $8.3 \times 10^8\,m^3$. Spatially, the pan-South Branch was net eroded by $9.7 \times 10^8\,m^3$ whereas the mouth bar zone was net deposited by $18 \times 10^8\,m^3$, suggesting that the mouth bar zone is a major sediment sink. Over time there is no directional deposition or erosion trend in the interval though riverine sediment supply has decreased by 2/3 since the mid-1980s. We infer that the pan-South Branch is more fluvial-controlled therefore its morphology responds to riverine sediment load reduction fast while the mouth bar zone is more controlled by both river and tides that its morphological response lags to riverine sediment supply changes at a time scale > 10 years, which is an issue largely ignored in previous studies. We argue that the time lag effect needs particular consideration in projecting future estuarine morphological changes under a low sediment supply regime and sea-level rise. Overall, the findings in this work can have implications on management of estuarine ecosystem, navigation channel and coastal flooding in general.

1. Introduction

Morphological evolutions are critical for socio-economic and ecological environmental development, especially in estuaries where most of the world's famous mega cities and harbors locate. The combined action of fluvial discharge, tidal flows, and waves generally controls the long-term estuarine morphological changes, resulting in a feedback loop between estuarine morphology and hydrodynamics through sediment transport (Cowell and Thom, 1994; Freire et al., 2011; Wang et al., 2013). Morphological evolution of large estuaries influenced by more than one primary forcing are insufficiently understood owing to inherent complexity in terms of large space scale and strong spatial and temporal variations. In addition, anthropogenic activities, such as waterway regulation project, dredging, embankment, reclamation, and dam construction, have profound effects on estuaries and human interventions play an increasingly important role in driving estuarine morphological changes (Milliman et al., 1985; Syvitski et al., 2005; Wang et al., 2013). Centennial bathymetric data of estuaries are rare while data at decadal time scales are readily more available, enabling quantitative examinations of medium- to long-term (decades to centuries) estuarine morphological evolution in response to natural forcing and human influences.

Morphological evolution and channel pattern changes in rivers, tidal basins, estuaries, and coasts have been broadly discussed at varying time scales. The depositional and morphologic patterns can be quite different under varying single or multiple primary forcing

* Corresponding author.
E-mail address: lcguo@sklec.ecnu.edu.cn (L. Guo).

https://doi.org/10.1016/j.jmarsys.2018.01.007
Received 4 May 2017; Received in revised form 17 January 2018; Accepted 19 January 2018
Available online 02 February 2018

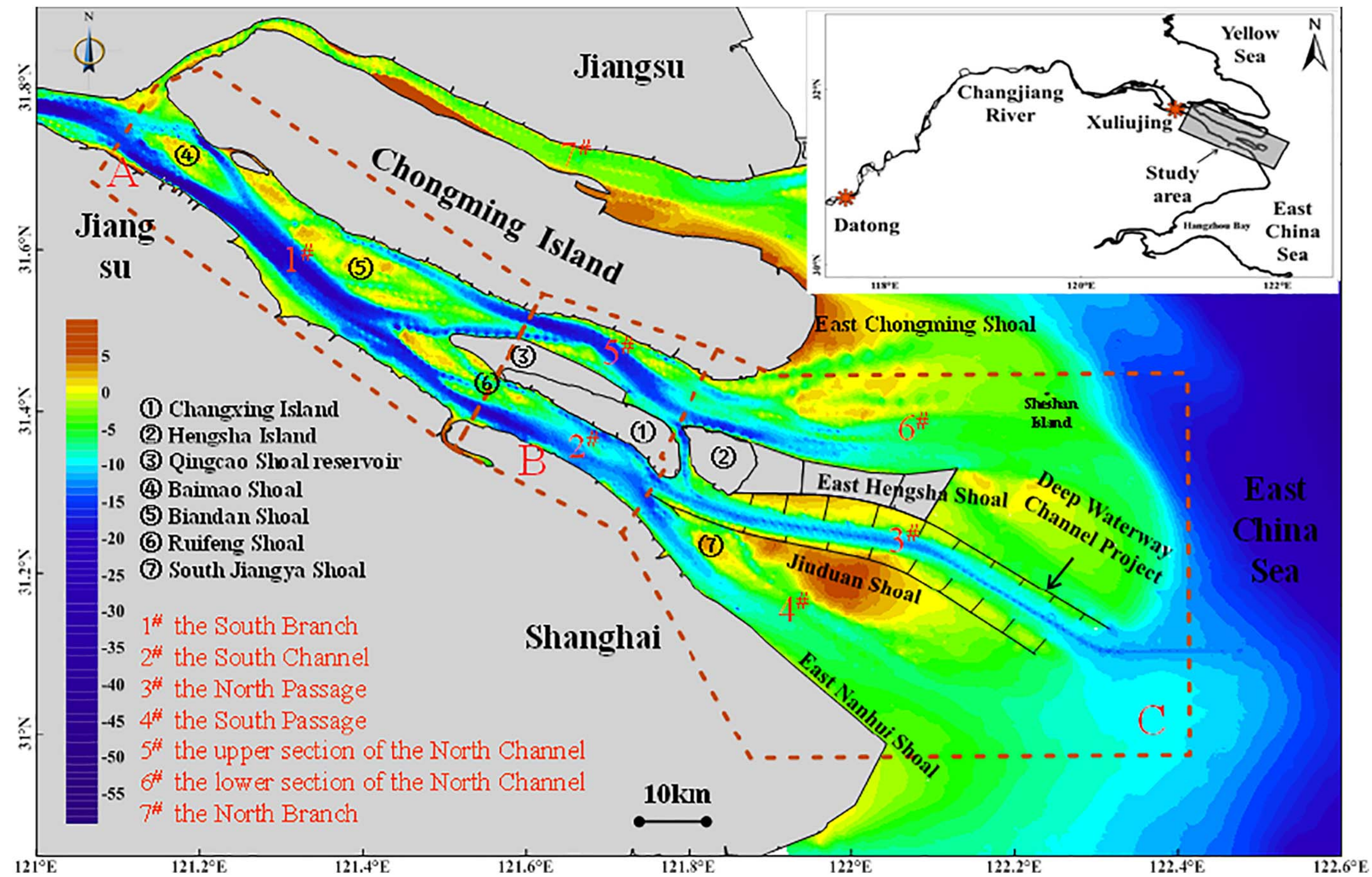

Fig. 1. A sketch map of the study area and division of different branches in the Changjiang Estuary with its bathymetry (depth in meters) in 2016. The whole study area is divided into three parts by brown solid lines, i.e., region A (the South Branch (1#)), region B (the South Channel (2#) and the upper section of the North Channel (5#)), and region C (the North Passage (3#), the South Passage (4#), and the lower section of the North Channel (6#)). (For interpretation of the references to colour in this figure legend, the reader is referred to the web version of this article.)

including river, tides, waves, etc. (Wright, 1977). A meandering channel pattern with coexisting flood and ebb channels is observed in tide-dominated systems, such as the Dutch Western Scheldt Estuary (Van Veen et al., 2005; Van den Berg et al., 1996; Toffolon and Crosato, 2007) and the Chesapeake Bay in the USA (Ahnert, 1960). Distributary channels with multiple bifurcations are observed in river-controlled estuaries and/or delta systems (Andrén, 1994; Edmonds and Slingerland, 2007; Wang and Ding, 2012). Large scale morphodynamic behavior under combined river and tidal forcing, such as the Changjiang Estuary in China, is insufficiently examined (Guo et al., 2014, 2015).

Morphological evolution of the Changjiang Estuary has been examined by calculating erosion-deposition volumes and analyzing movements of isobaths, shorelines, and thalwegs (Chen et al. 1985 and 1999; Yun, 2004; Wang et al., 2013; Luan et al., 2016). Riverine sediment source availability and human activities are widely seen as two important factors in controlling morphological evolution in the Changjiang Estuary, which is also true in other estuaries and deltas such as Niles, Mississippi, and Colorado (Syvitski and Kettner, 2011). Note that previous examinations of the morphological changes in the Changjiang Estuary were mainly at regional scale without taking the estuary as a whole into consideration. For instance, owing to riverine sediment supply reduction, regional erosion was detected in the South Branch (Wang et al., 2013) and the delta front regions (10 m deep nearshore) (Yang et al., 2003, 2005, 2011) in the recent decades, whereas the examination of a larger region including the sand bars in the mouth bar zone indicates continued deposition (Dai et al., 2014). Moreover, the time scale of large scale estuarine morphodynamic adaptation in responding to external forcing changes is very much ignored in previous studies. The morphological impacts of human activities such as reclamations (Chu et al., 2013; Wei et al., 2015) and the Deep Waterway Channel Project along the North Passage (De Vriend et al., 2011; Jiang et al., 2012, 2013) can also vary in a large space and time scales depending on their location, implementation time, and scales. Sea-level rise is also another factor needs consideration (Wang et al., 2013; Wang et al., 2014; Wei et al., 2015). So far, a comprehensive and quantitative investigation of morphological evolution in the entire Changjiang Estuary is still very much needed.

This study analyzes the morphological changes in the Changjiang Estuary as a whole based on the bathymetric data collected in the period between 1958 and 2016. We will focus on the erosion-deposition processes, changes of hypsometry, and cross-section configuration of different branches in the estuary to elaborate the channel patterns and the spatial and temporal variability of the estuarine morphology. The controls of the morphological changes are discussed in terms of natural processes and human activities. The insights obtained from this study are helpful for management and restoration opportunities in the Changjiang Estuary.

2. Data and methods

2.1. Brief introduction to the Changjiang Estuary

The Changjiang River and its estuary is one of the biggest on earth with respect to its quantity such as river discharge, sediment load, and space scales. The annual mean river discharge is approximately $28.3 \times 10^3\ m^3/s$ (1950–2015) and annual sediment load is 3.7×10^8 tons (1953–2015) (CWRC, 2015). The river and sediment

Table 1
Annual mean river discharge and sediment load at Datong and the erosion or deposition parameters (net rates, area and net thickness) in region A, B, C, and whole study area (A + B + C) during different periods (1958–1973, 1973–1986, 1986–1997, 1997–2002, 2002–2010, 2010–2016) (positive values stand for deposition while negative values stand for erosion).

	Location		Unit	1958–1973	1973–1986	1986–1997	1997–2002	2002–2010	2010–2016
Annual-mean	Datong	River discharge	10^8 m^3/year	8632	8925	8805	10,018	8401	8588
Annual-mean	Datong	Sediment load	10^8 t/year	4.88	4.53	3.60	3.36	1.84	1.28
Erosion/deposition parameters	Region A	Net rates	10^6 m^3/year	19.2	−0.4	−35.9	16.0	−37.7	−28.8
		area	10^8 m^2	6.9	6.8	6.6	6.7	6.3	6.3
		Net thickness	mm/year	27.7	−0.5	−54.3	23.9	−59.6	−45.8
	Region B	Net rates	10^6 m^3/year	5.5	−11.1	8.4	−23.5	−23.7	−31.7
		Area	10^8 m^2	3.6	3.6	3.5	3.5	2.9	2.9
		Net thickness	mm/year	15.1	−31.1	24.4	−67.8	−81.9	−110.8
	Region C	Net rates	10^6 m^3/year	73.5	2.3	83.7	−32.5	75.3	−115.3
		Area	10^8 m^2	29.0	28.9	28.6	27.9	27.3	25.4
		Net thickness	mm/year	25.3	0.8	29.3	−11.6	27.6	−45.3
	A + B + C	Rates	10^6 m^3/year	98.2	−9.2	56.3	−40.0	13.9	−175.7
		Area	10^8 m^2	39.6	39.3	38.7	38.1	36.5	34.6
		Thickness	mm/year	24.8	−2.3	14.5	−10.5	3.8	−50.8

discharges exhibit markedly seasonal variations, with about 71% of water flux and 87% of sediment load flushed in the wet season between May and October (Chen et al., 2007). Mean tidal range decreases from about 3.2 m nearshore to 2.4 m at Xuliujing, the present delta apex, and further to be insignificant 500 km upstream of Xuliujing. The tidal prism varies between 1.3×10^9 and 5.3×10^9 m^3, with a mean tidal discharge almost 9 times as much as the mean river discharge (Chen and Li, 2002). Thus the Changjiang Estuary is dominantly a partially-mixed, meso-tidal system (Chen and Li, 2002). The waves in the Changjiang Estuary are mainly wind waves with a mean wave height of 0.9 m at Yinshuichuan in the river mouth area (Wu et al., 2009; Wang et al., 2013). River and tides are the main forcing conditions though wind and waves can affect hydrodynamics and sediment transport over the shallow tidal flats. The present Changjiang Estuary has four prime inlets connecting to the sea, namely the North and South Branch, North and South Channel, and North and South Passages (Fig. 1). The estuary mouth is as wide as 90 km and the width decreases to approximately 6 km at the apex of the funnel-shaped estuary, i.e., Xuliujing. Overall the Changjiang Estuary is a complex large scale system with few comparable cases in the world.

2.2. Data and methods

We collect bathymetric data in 1958, 1973, 1986, 1997, 2002, 2010, and 2016, covering the entire regions seaward Xuliujing until 10–15 m deep waters (Fig. 1). The North Branch (NB), nowadays tide-dominated and limitedly influenced by fluvial processes, is excluded in this study due to data scarcity. The bathymetry data in 1958, 1973, and 1986 are obtained from digitization of historical marine charts with a resolution 1/50000 and data in other years are from field sounding measurements with an accuracy of 1–2% for depths < 2 m and < 1% for depths > 2 m (Wang et al., 2011, 2013). All depth data are referenced to the same datum, the Theoretical Lowest Astronomical Tide (TLAT), which is basically below local mean water level by a half maximum tidal range (~2 m). A digital elevation model (DEM) by 20×20 m is created using Kriging interpolation.

Considering spatial variations of hydrodynamics, sediment properties, and morphological features (Fig. 3), we divide the study area into three regions for the benefit of clarification. Region A includes the South Branch (SB) and region B includes the South Channel (SC) and the upper section of the North Channel (NC), while region C indicates the mouth bar zone (MBZ) which includes the lower section of the North Channel, the North Passage (NP), and the South Passage (SP). Regions A and B together are also named pan-South Branch (PSB) region as a counterpart of region C (Fig. 1). Erosion and deposition volumes of different regions and the estuary as a whole are calculated for different time intervals. Hypsometry curves are also derived by linking channel volumes and planar areas at different depths. The hypsometric curves help to uncover morphological change of channels and shoals in the vertical direction. Moreover, we also estimate variations of width, depth, and width-to-depth ratio and examine cross-section profile variations in different regions.

3. Results

3.1. Overall morphological evolution (1958–2016)

We see that there is no new channel bifurcation in the Changjiang Estuary since 1958. The three-level bifurcation and four-outlet configuration persists and the channels and shoals develop toward mature conditions by strong erosion and deposition evolution (Fig. 4). The middle-channel channel-shoal pattern is featured by meandering channels and sand bars. The entire estuary becomes narrower and deeper owing to deposition over the shoals and tidal flats and erosion along the channels.

3.2. Erosion and deposition patterns

The study area as a whole (including regions A, B, and C) had experienced deposition from 1958 to 2016. The total net deposition amount of the study area reached 8.3×10^8 m^3 over 59 years, which equals a net deposition rate of 14.3×10^6 m^3/year.

Temporally, the estuary did not exhibit directional persistent deposition or erosion over 59 years (Table 1, Fig. 4). The entire study area first experienced fast deposition in 1958–1973 (98.2×10^6 m^3/year), followed by slight erosion in 1973–1986 (9.2×10^6 m^3/year), deposition in 1986–1997 (56.3×10^6 m^3/year), erosion in 1997–2002 again (40×10^6 m^3/year), slight deposition in 2002–2010 (13.9×10^6 m^3/year), and recently fast erosion in 2010–2016 (175.7×10^6 m^3/year).

Spatially, the net erosion volume was 9.7×10^8 m^3 in the pan-South Branch between 1958 and 2016. Approximately 52% of that occurred in region A and 48% in region B. To the contrast, the MBZ was deposited by 18×10^8 m^3 in the interval, indicating that the MBZ is a major sediment sink. The erosion and deposition patterns are different in different regions (Table 1). Region A had changed from deposition (1958–1973, 19.2×10^6 m^3/year) to erosion (2010–2016, 28.8×10^6 m^3/year). Similar variation behavior was also observed in region B by slight deposition (1958–1973, 5.5×10^6 m^3/year) and moderate erosion (2010–2016, 31.7×10^6 m^3/year). However, region C showed a strong deposition trend from 1958 to 2010 and the deposition rates reached up to 75×10^6 m^3/year most of the time, followed by significant erosion of 1.15×10^8 m^3/year since 2010.

3.3. Changes of hypsometry

Hypsometric curve is a concise and quantitative way to understand vertical morphological characteristics. According to the hypsometric curves of the study area as a whole from 1958 to 2016 (Fig. 5D), both the total water volume and area of the study area decreased due to deposition and human activities. Specifically, the total water volume of the region below $+2$ m isobaths was $31.6 \times 10^9\,m^3$ in 1958. It decreased to $30 \times 10^9\,m^3$ in 2016, indicating 5% reduction compared to 1958. The total area at $+2$ m isobaths also decreased by about 514 km^2 from 1958 to 2016, i.e., 13% of that in 1958, mainly owing to reclamations and embankment for the Qingcao Shoal reservoir.

In the vertical direction, the erosion and deposition patterns of the sand bars and shoals and the deep channels were quite different from each other during the past 59 years. By comparing the water volumes and areas of the channels under different isobaths in both 1958 and 2016 (Fig. 5D), we see that the entire study area was confined by -8 m isobaths. The water volume of the region above -8 m ($-8\sim+2$ m) isobaths reduced from $28.1 \times 10^9\,m^3$ in 1958 to $25 \times 10^9\,m^3$ in 2016, and the area decreased from $2.76 \times 10^9\,m^2$ to $2.15 \times 10^9\,m^2$. Deposition took place in the sand bars and shoals, which includes intertidal zone ($0\sim+2$ m). The water volume of the region below -8 m isobaths ($-8\sim-20$ m) increased by about $1.49 \times 10^9\,m^3$ and the area increased by $0.1 \times 10^9\,m^2$. In the deep part of the channels below -12 m isobaths, the water volume and the area increased by $0.9 \times 10^9\,m^3$ and $0.11 \times 10^9\,m^2$, respectively. Thus the channels, especially the deep parts of them, were continuously eroded from 1958 to 2016.

For three regions of the estuary, deposited sand bars and shoals and eroded deep channels were also detected from 1958 to 2016, but the depth thresholds for shallow (deposited) and deep (eroded) areas were different. Region A as a whole was separated by -7 m isobaths while region C was separated by -8 m isobaths. The shape of the hypsometric curves in different years was similar to each other, for both regions A and C (Fig. 5A and B). However, region B was separated by -1 m isobaths. The hypsometric curves in region B had significantly changes during the past 59 years, especially after 2002, mainly owing to embankment for the Qingcao Shoal reservoir (Fig. 5C).

3.4. Changes of cross-section

The width of the cross-sections in region C increases in the seaward direction. The depth of the cross-sections has a significant seaward decrease trend and has a minimum value on the top of the mouth bar. They are quite different from those in regions A and B which do not have such a significant seaward depth variation along the river.

For the chosen 6 cross-sections in the Changjiang Estuary (Fig. 6), the width and average depth at 0 m of the cross-section 1 in region A were 11.1 km and 8 m in 1958, respectively. They changed to 11.5 km and 8.6 m in 2016. And the width to depth ratio (B/H) reduced by 4% from 1958 to 2016. The average depths of the cross-sections 2 and 3 in region B both increased by 0.2 m and 3.1 m, respectively. The width of the former increased by about 5% while the latter reduced by 16%. The B/H of the cross-section 2 in the South Channel had no obvious change, but that of the cross-section 3 in the upper section of the North Channel significantly decreased by 40%, due to embankment for the Qingcao Shoal reservoir. The above-mentioned parameters of cross-sections 4, 5 and 6 in region C also had a similar variation tendency as those in the upper section of the North Channel. From 1958 to 2016, the mean width and width to depth ratio of the three cross-sections in region C reduced by 42% and 60%, respectively, while the mean depth increased by almost 50%. The reclamations in both East Nanhui shoal and East Hengsha shoal and the Deep Waterway Channel Project in the North Passage were the main reasons for such changes (Fig. 6B and C).

So far, the width at 0 m of the most cross-sections in the Changjiang Estuary had a decreasing trend while the average depth had an increasing trend from 1958 to 2016, especially in the regions where human activities occurred frequently. Thus the mean width to depth ratio of the cross-sections decreased obviously during the past 59 years. It indicated that the cross-sections in the Changjiang Estuary became much narrower and deeper from 1958 to 2016, corresponding to deposition in the sand bars and shoals and erosion in the deep channels.

4. Discussion

4.1. Spatially varying hydrodynamics and sediment characteristics

The Changjiang Estuary covers so large area that hydrodynamics and sediment transport dynamics present strong spatial variations from upstream to downstream due to the combined effect of river and tides (Liu et al., 2010; He et al., 2015). Most of the main channels in the Changjiang Estuary are ebb-dominated with stronger ebb currents than flood currents (Fig. 3A). The ratios of river discharge to tidally mean discharge (Q_r/Q_t) present an obvious decreasing tendency in the seaward direction. For instance, the Q_r/Q_t ratios are 0.44 and 0.12 in regions A and C, respectively (Fig. 3B). From the South Branch to the MBZ, the Q_r/Q_t ratio reduces by 73%. It indicates that the South Branch is more river-influenced while the MBZ is much more tidal-influenced than the South Branch.

The suspended sediment concentration (SSC) exhibits an increasing trend from upstream (region A) to downstream (region C). For example, the mean SSC was only 0.43 kg/m^3 between 2003 and 2007 in the South Branch (region A), while the mean SSC increased to 0.99 kg/m^3 in the South Passage (region C), which is twice more than that in the South Branch (Fig. 3C; Liu et al., 2010; He et al., 2015).

The grain size of suspended sediment presents an increasing trend from the South Branch to the MBZ (Fig. 3D). In 2003, the median grain size of suspended sediment in region A was 6.5 μm while it was 8–9.5 μm in the MBZ. In contrast, the grain size of bottom sediments decreases seaward along the river. In the main channel of the South Branch, the median grain sizes of bottom sediments were > 200 μm while such values were far $^{<}$50 μm in the main channel of the MBZ in 2003 (Fig. 3E).

All these differences between regions A and C (region B is in transition between them) suggest that they are controlled by different hydrodynamic conditions thus potentially explaining different morphological behavior between them.

4.2. Spatially varying morphodynamic behavior of the Changjiang Estuary

Riverine input is a major source of water and sediment fluxes that influence the estuarine morphological evolution. Sediment source reductions below pristine conditions are observed in many estuaries creating new challenges to estuaries and deltas under sea level rise (Syvitski and Kettner, 2011). For the Changjiang Estuary, it was obvious that the morphological changes were influenced by riverine sediment load reduction (Yang et al., 2005, 2011; Kuang et al., 2013; Wang et al., 2008, 2013; Wang et al., 2014), but some parts of the estuary, such as the MBZ, had little response to riverine sediment load reduction within a short time (Dai et al., 2014), owing to the complex spatio-temporal variations of hydrodynamics and sediment characters in such a large estuary. The effects of sediment source reduction caused by the Three Gorges Dam in the watershed on estuarine morphological change are still in dispute. How different branches in the Changjiang Estuary responded to sediment source reduction needs further clarification.

It is widely known that river discharge acting on the Changjiang Estuary did not show significant decreasing or increasing trend from 1958 to 2016, but the sediment load at Datong had significantly reduced since the mid-1980s, mainly attributed to dam constructions in the drainage basin. The annual river discharge at Datong remained about $890 \times 10^9\,m^3$/year in the total six periods while the annual sediment load had continuously reduced from 4.82×10^8 t/year

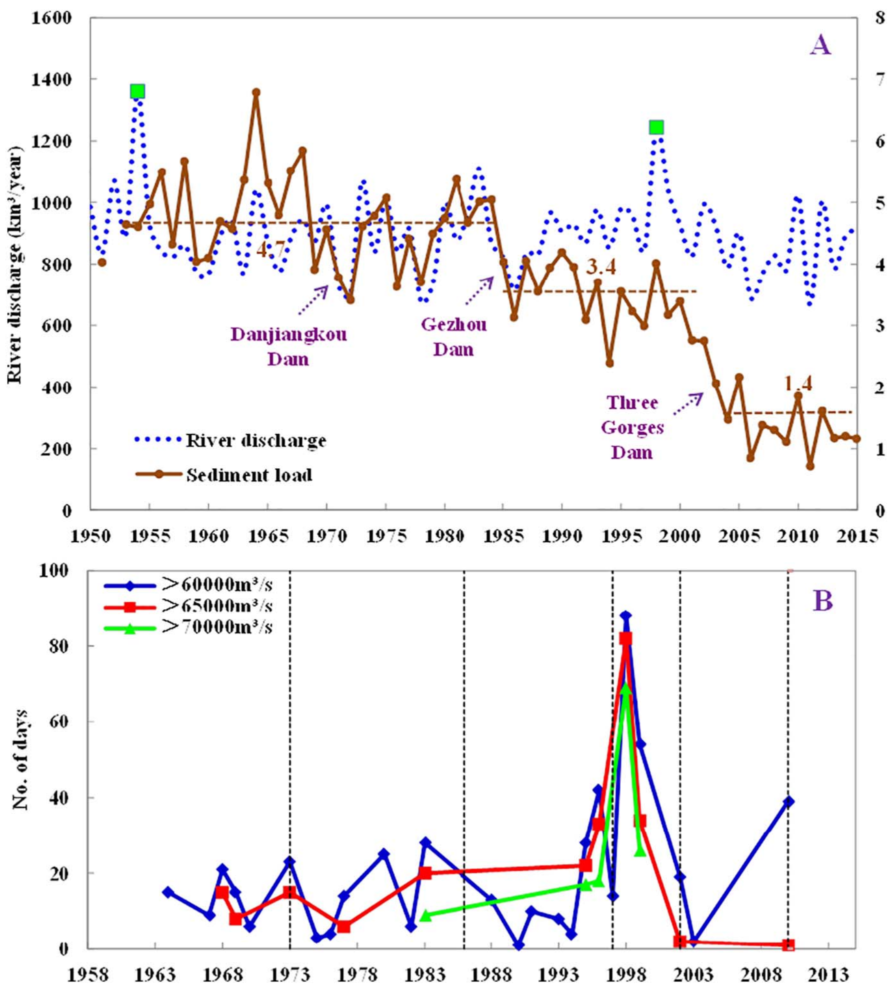

Fig. 2. (A) Annual river discharge and sediment load at Datong from 1950 to 2015 (Blue dotted line: annual river discharge from 1950 to 2015, Brown solid line: annual sediment loads from 1951 to 2015, Brown dotted lines: the annual mean sediment loads during different periods which indicated the riverine sediment load reduction mainly due to dam constructions in the Changjiang River basin (4.7×10^8 t/year 1953–1984, 3.4×10^8 t/year 1986–2002, 1.4×10^8 t/year 2004–2015), Green square solid points: the years that catastrophic floods happened in both 1954 and 1998). (B) The number of the days that daily water discharge is > 60,000 m^3/s (blue), 65,000 m^3/s (red), and 70,000 m^3/s (green) each year at Datong from 1958 to 2015. (For interpretation of the references to colour in this figure legend, the reader is referred to the web version of this article.)

(1958–1973) to 1.28×10^8 t/year (2010–2016), a 2/3 reduction (Fig. 2A; Chen et al., 2008; He et al., 2015). However, there was no directional deposition or erosion trend of the entire study area in the estuary (Table 1), suggesting that estuarine morphological changes are not linearly or simply correlated with riverine sediment supply changes as widely documented in previous studies. We will discuss potential factors acting on the inconsistent change behavior, including spatially varying estuarine morphological response behavior, time lag effect, etc.

Both regions A and B were featured by an obvious switch change from deposition to erosion over time. A positive linear relationship was found between the annual mean erosion or deposition rates in region A ($R^2 = 0.48$) and region B ($R^2 = 0.56$) and the annual mean sediment load at Datong (Fig. 7A and B), indicating that the morphological changes of these two regions had a good relationship with riverine sediment source variations. We infer that the pan-South Branch is more fluvial-influenced that its morphology is sensitive to riverine sediment supply reduction. On the other hand, the MBZ presented a persisting deposition trend prior 2010 and turned to be afterward erosion. The annual mean erosion or deposition rates of the MBZ had poor relationship with the annual mean sediment load at Datong over 59 years ($R^2 = 0.19$) (Fig. 7C). We think the MBZ is controlled by both river and tides that its morphological changes can have resilience to sediment source changes and/or are out of phase of sediment source changes.

Specifically, region A turned to be moderately eroded from 1986 to 1997, but region B still showed a slight deposition at that time and shifted to moderate erosion from 1997 to 2002. The response of the South Branch and region B to riverine sediment source reduction thus did not occur simultaneously. We see that both the mean annual erosion or deposition rates of region A and region B are positively correlated to the annual mean sediment load at Datong, suggesting erosion happened in these zones due to riverine sediment source reduction. For region A, the correlationship changes little ($R^2 < 0.48$) when considering a 2 year time lag between estuarine morphology and riverine sediment supply. The correlationship significantly improves ($R^2 = 0.77$) in region B considering a time lag of 5 years (Table 2). It indicates that there is a $^{>}5$ years of time lag for the response of morphological changes in

Table 2
Linear correlation coefficients between the mean annual erosion/deposition rates in region A (A) (i.e., the South Branch), region B (B), and region C (C) (i.e., the MBZ) and the mean annual sediment load at Datong in current periods or 1–5 years before the current periods.

R^2						
Region	Corresponding year	Previous 1 year	Previous 2 years	Previous 3 years	Previous 4 years	Previous 5 years
A	0.48	0.48	0.45	0.35	0.28	0.23
B	0.56	0.58	0.63	0.71	0.73	0.77
C	0.19	0.23	0.29	0.38	0.51	0.53

region B, while the time lag of region A is in the order of ~2 years, which is shorter than that in region B. The annual mean erosion or deposition rates of region C (the MBZ) has little ($R^2 = 0.19$) relationship with the annual mean sediment load at Datong. The correlationship also improves ($R^2 = 0.53$) considering a time lag of 5 years (Table 2). Though limited data about sediment load at Datong before 1953 is available, we believe that the time lag of morphological changes in the MBZ can be > 10 years considering its large scale and tidal influence.

The presence of a time lag between large scale estuarine morphological responses to riverine sediment supply variations is understandable. The Changjiang Estuary is primarily controlled by river and tides. River discharge transports a large amount of suspended sediment seaward and flushes bottom sediments downward. Tidal waves and currents propagate landward and create stratification and gravitational circulations particularly in region C, which have effects in trapping sediment in the mouth bar (turbidity maximum zone) and even inducing landward sediment transport in the bottom layers. Tidal asymmetry and tidal pumping can also favor landward sediment transport though it may be of secondary importance due to high river discharge (Guo et al., 2014, 2015). Sediment redistribution within the estuary, e.g., by channel erosion and flat accretion, explains the large scale morphological resilience to external source changes (Guo, 2014). Spatially, region A is overall well-mixed and more river-influenced and its sediment source and transport processes are directly affected by river forcing first (He et al., 2015), explaining why the South Branch is sensitive to riverine input and a small time lag. Region C is dominantly partially-mixed and both river and tides are of equal importance. Region C is strongly affected by density currents, horizontal circulations, tidal asymmetry, etc. (Guo, 2014; Wu et al., 2010, 2012; Jiang et al., 2013), that its morphology has large resilience and inherent buffering effects to riverine sediment source changes. Region C, facing to the open sea, is also influenced by wind and waves which can rework tidal flats sediments to be transported and deposited in channels. Overall these processes explain why a large time lag is present in the MBZ compared to the inner estuary, e.g., the South Branch.

The time scale of sediment transport in such a large estuary system may also play a role though it is difficult to quantify accurately. The riverine sediment flux monitored at Datong, 600 km upstream of region C, may take quite a while to be transported seaward step by step while along river morphological changes have buffering effects. It can explain the seaward increasing time lag. The SSC in both regions A and B had decreased significantly over time. For instance, the depth-averaged SSC in the South Branch and the South Channel reduced by 84% and 64% from 2003 to 2013, respectively (Fig. 3C). However, the depth-averaged SSC in the MBZ was still high (> 0.5 kg/m^3) and even increased by 36% in the North Passage and 75% in the lower section of the North Channel (Fig. 3C). It suggests that the response behavior in region C is quite different from regions A and B.

The overall erosion since 2010 in all the three regions may suggest that the estuary undergoes a shift from overall deposition to erosion after a time lag (Fig. 4, Table 1). Comparing with the previous period (2002 – 2010), the erosion rate of region A decreased while the erosion rate of region B increased (Table 1). However, the MBZ sustained a high deposition rate from 2002 to 2010, even the sediment load at Datong had reduced by 2/3 since 2003. It suggests that the effects of riverine sediment source reduction on the MBZ are only detectable in the very recent years. It again supports the argument of a time lag $^>$10 years for the response of the morphological changes in region C to riverine sediment source reduction. The time lag effect is easily ignored in the morphological examination in previous studies, which can explain why the controversial conclusions reached.

So far the time lag is only quantitatively discussed due to large bathymetric data interval. Future work by morphodynamic modeling can help to better quantify the time lag and its spatial variability. Actually a large estuarine morphodynamic adaptation time scale is reported in schematized long-term estuarine and deltaic morphodynamic studies and it merits careful consideration in real world as well when predicting future morphological changes in response to a low sediment influx regime and sea level rise.

4.3. Spatially varying morphological changes under big river floods

Estuarine morphological evolution is so complex that it is influenced by a variety of factors other than riverine sediment load changes. River flow is just one prominent process governing estuarine morphodynamics. Though the annually mean river discharge changes little and is not expected to cause directional estuarine morphological changes (Table 1), changes of the frequency and magnitude of episodic big river floods can play a role in shaping morphological evolution (Yun, 2004; Guo, 2014; Luan et al., 2016). At long-term time scales, catastrophic river floods with a peak river discharge $^>$70,000 m^3/s were thought to play an prominent role in stimulating new channel bifurcation in the Changjiang Estuary, such as the formation of the North Passage due to the big flood in 1954 (Yun, 2004). At decadal time scales, we identify five years with flood peak discharges $^>$70,000 m^3/s from 1958 to 2016, including a catastrophic flood in 1998. We see that most of the high river discharges occurred in the period of 1997–2002 (Fig. 2B). Accordingly, the estuary displayed severe erosion in the same interval (1997–2002) compared to other periods though net deposition was detected in region A due to the accretion over the shoals (Fig. 4). This change pattern was inconsistent with the long-term tendency between 1958 and 1997 (Table 1). Linear riverine sediment source reduction since the mid-1980s failed to explain such intense changes.

We argue that enduring high river discharges exert strong influence on estuarine morphological changes. The high river discharges (> 70,000 m^3/s) persisted 1–2 months in 1998 and 1999, and post-flood discharges maintained at a relatively high level (> 45,000 m^3/s) for 2–3 months in these two years. The river discharge hydrographs were quite different from normal conditions. It provided a continuous strong river force in flushing sediment seaward. Moreover, based on the historical data from 1951 to 1984, Yin and Chen (2009) found significant sediment deficiency for river discharges > 60,000 m^3/s at Datong. High river flow has a larger sediment transport capacity but the sediment source-limited condition in the river upstream Datong restricts sediment availability to the estuary, thus triggering erosion in the estuary considering further by enhanced sediment transport capacity thru river-tide interactions (Guo, 2014). The net deposition in region A in 1997–2002 reflects the imbalance between channel erosion and shoal accretion which is very much related to channel migration and shoal movement caused by big river floods as well. Overall we think that it is not only the magnitude of the flood peak discharges, but also its duration and associated sediment deficiency, matter in causing strong estuarine morphological changes.

4.4. The influence of human activities

Extensive human activities in the estuary locally, such as the Deep Waterway Channel Project, dredging, reclamation, and embankment for reservoir construction, also exert strong impacts in estuarine morphological evolution at decadal time scales (Fig. 8A).

Reclamation and embankment is one of the main factors in stabilizing coastlines and narrowing channels in historic periods. The width of the Xuliujing section narrowed from 15.7 km in 1958 to 5.7 km in 1970s due to reclamation and the narrowed Xuliuing section became a controlling point in stabilizing the division between the South Branch and the North Branch (Yun, 2004; Guo, 2014). As a result of it, the old Baimao Shoal moved northward and merged with the Chongming Island in 1970s and the entrance of the South Branch became much narrower and deeper from 1958 to 1973. For the entire study area, a reduction of 571 km^2 of the water surface area resulted from reclamation and embankment from 1958 to 2016, accounting for almost 14% of

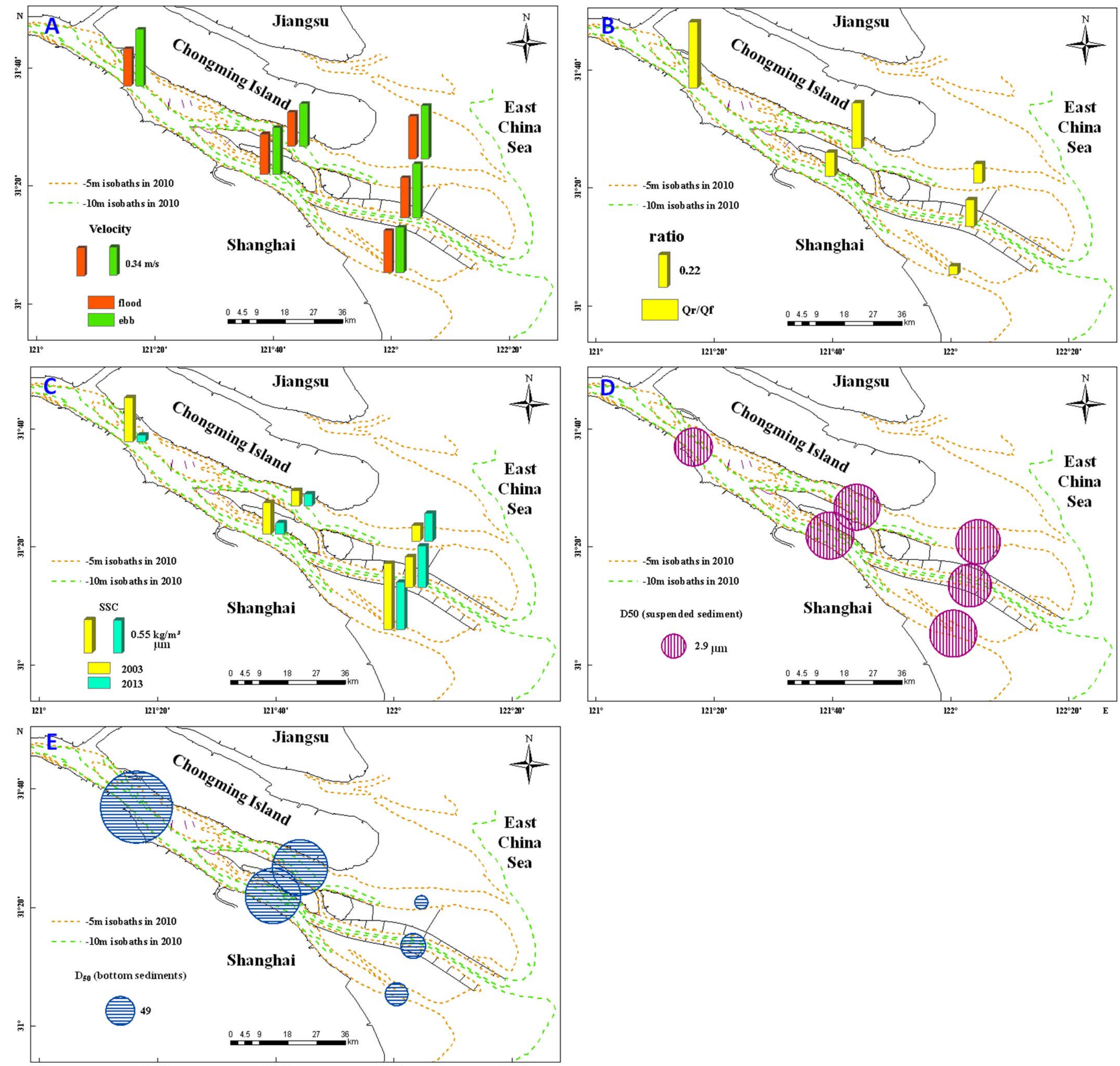

Fig. 3. Longitudinal distribution of the depth-averaged flood and ebb current velocity during a neap-spring tidal cycle (A), ratio of river discharge to tidally mean discharge (Q_r/Q_t) during a neap-spring tidal cycle (B), depth-averaged suspended sediment concentration (C) (yellow bar: 2003; blue bar: 2013), depth-averaged suspended sediment D_{50} (D), and bottom sediments D_{50} (E) in wet season in 2003 (data from Liu et al., 2010 and He et al., 2015). (For interpretation of the references to colour in this figure legend, the reader is referred to the web version of this article.)

that in 1958, which meant 11 man-made Hengsha Islands formed in the Changjiang Estuary (Fig. 8A). Due to the reclamation and embankment, the channels in the estuary become much narrower and deeper, especially around the regions reclamation or embankment occurred nearby. For instance, the width and width to depth ratio of the cross-section 3 obviously decreased by 16% and 40%, respectively, especially after 2009 owing to embankment for the Qingcao Shoal reservoir (Fig. 6).

The Deep Waterway Channel Project was carried out in the North Passage of the Changjiang Estuary since 1998 and almost 50–80 × 10^6 m^3 of sediment was dredged each year from the navigation channel (Fig. 8B). The morphological changes of the MBZ, including the North Passage, were intensely impacted by these human interventions. The North Passage tended to be a man-controlled bifurcation channel owing to the navigational works and dredging. The cross-section of the North Passage also became narrower and deeper. Taking cross-section 5 as an example, a 53% reduction in width and a 35% growth in average-depth were observed from 1958 to 2016 and a dramatic change mainly occurred since 2002 because of the navigational works and dredging. Other changes such as local erosion in the middle reach of the North Channel and the upper section of the South Passage and reduced horizontal growth and enhanced vertical accretion of the Jiuduan Shoal from 2002 to 2010 were also attributed to the navigational works (Jiang et al., 2012).

Human activities play a more important role in driving abrupt changes of estuarine morphology by stabilizing coastlines and narrowing channels in relatively short time and their impacts can persist

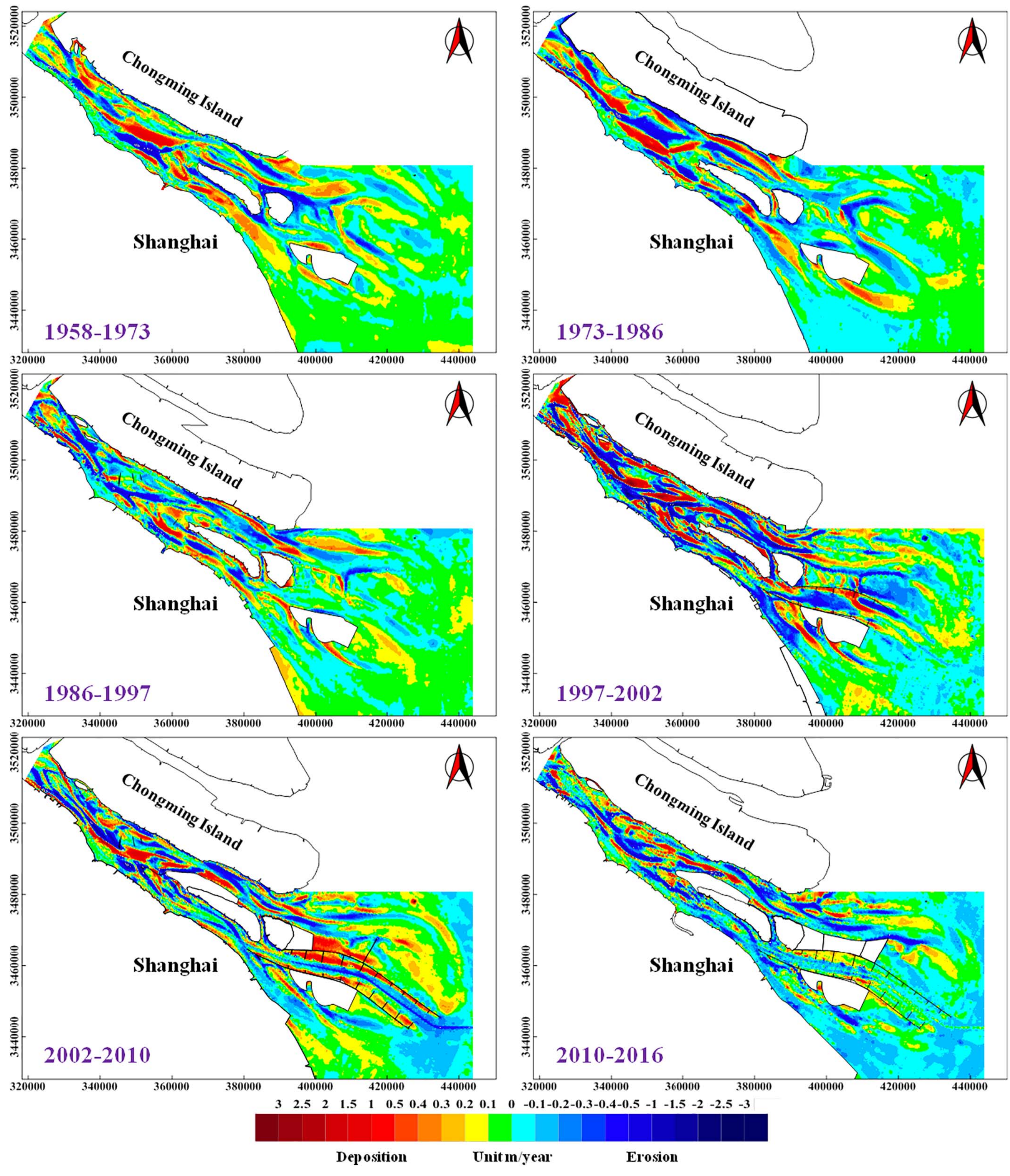

Fig. 4. Bathymetry changes of the study area during different periods (1958–1973, 1973–1986, 1986–1997, 1997–2002, 2002–2010, and 2010–2016) (unit: m/year).

for long time, overlapped by slow changes under natural evolution processes. Overall the Changjiang Estuary is becoming more constrained and human-influenced due to extensive reclamation, embankment, and navigational works and the channel-shoal system of the estuary will be more stabilized under human interventions in the future.

5. Conclusions

We analyzed and interpreted 59-year's morphological evolution of the Changjiang Estuary as a whole from 1958 to 2016 and inferred the causes and implications. We see that its channel-shoal pattern featured by meandering and bifurcated channels does not change over decades

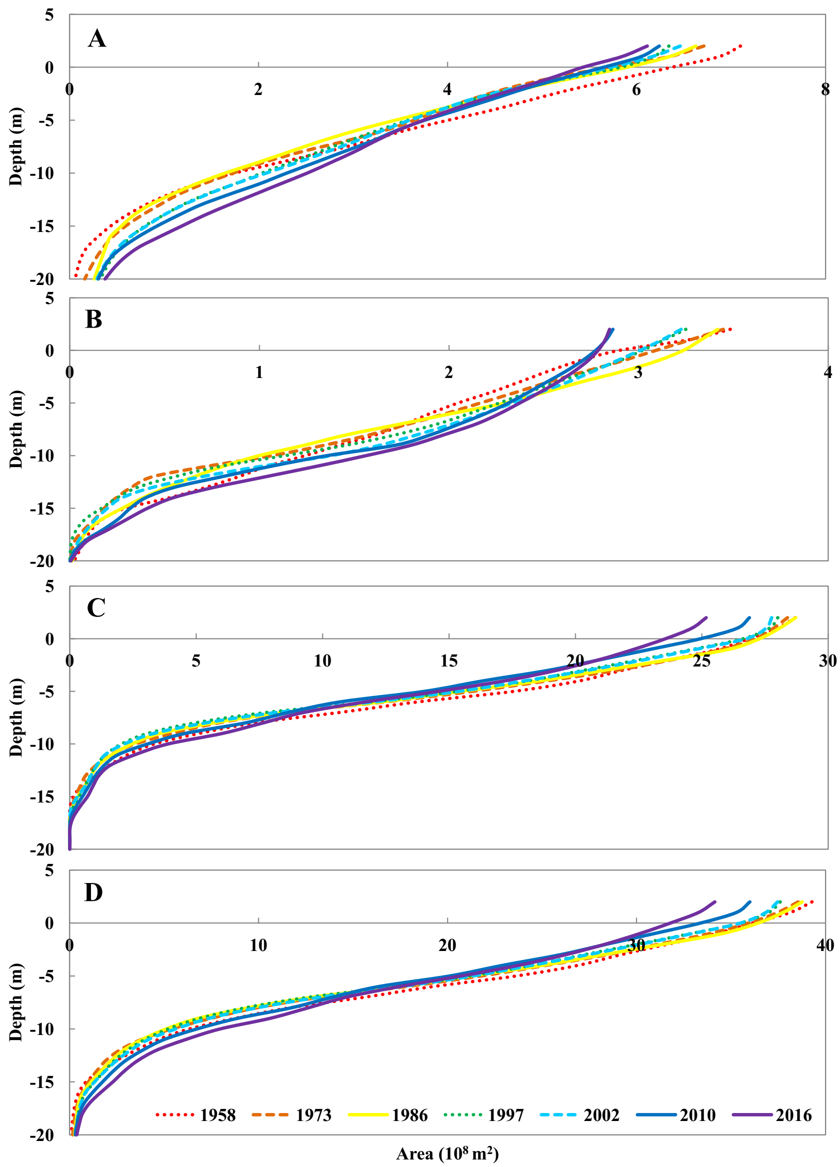

Fig. 5. Hypsometry changes of region A (A), region B (B), region C (C), and entire study area (D) from 1958 to 2016.

though there is strong erosion and deposition. The Changjiang Estuary exhibits an overall deposition trend but with strong temporal and spatial variations. The net deposition volume of the whole study area was $8.3 \times 10^8\,m^3$ from 1958 to 2016, or a net deposition rate of $14.3 \times 10^6\,m^3$/year.

Spatially both regions A and B, the inner part of the estuary, turned from deposition to erosion, i.e., by totally $5 \times 10^8\,m^3$ and $4.7 \times 10^8\,m^3$ eroded, respectively, over 59 years. However, there was $18 \times 10^8\,m^3$ of deposition in region C, i.e., the mouth bar zone, from 1958 to 2016. Erosion had been also detected since 2010 in the MBZ. The strong spatial variability can be explained by the differences in their hydrodynamic forcing and morphological features owing to along river distribution of river and tide energy. In the vertical direction, the hypsometric curves showed that deposition happened over the sand bars and shoals, whereas erosion mainly occurred in the deep channels since 1958. As a result, the channels of the estuary became much narrower and deeper.

The non-directional deposition and erosion trend of estuarine morphological changes is consistent with directionally decreasing riverine sediment supply. The morphological change of the pan-South Branch had a good relationship with riverine sediment source reduction. We infer that the pan-South Branch is more fluvial influenced and its morphology is sensitive to riverine sediment supply reduction. The mouth bar zone is controlled by both river and tides thus its morphology does not show a clear linkage with sediment supply. Seaward sediment flushing takes time and there is a time lag between estuarine morphological changes and riverine sediment source variations in the different regions. The time lag increases in the seaward direction and it is > 10 years in the mouth bar zone. Sediment redistribution has buffering effect and the estuarine circulation, tidal pumping, waves, etc. can also explain sediment trapping in the mouth bar zone which has a large morphological resilience to external source changes. We argue that the time lag effects need to be considered when examining large scale estuarine morphological changes in response to riverine sediment supply variations which is not well understood but an important issue given projection of future changes.

Big river flows with long duration and sediment deficiency may also explain the erosion in periods from the late 1990s to early 2000s.

Human activities such as the Deep Waterway Channel Project, reclamation, and embankment play an important role in driving morphological evolution in the estuary by stabilizing coastlines and narrowing channels. Overall the Changjiang Estuary is becoming more constrained and man-influenced due to extensive reclamation, embankment, and the navigational works and the channel-shoal system of

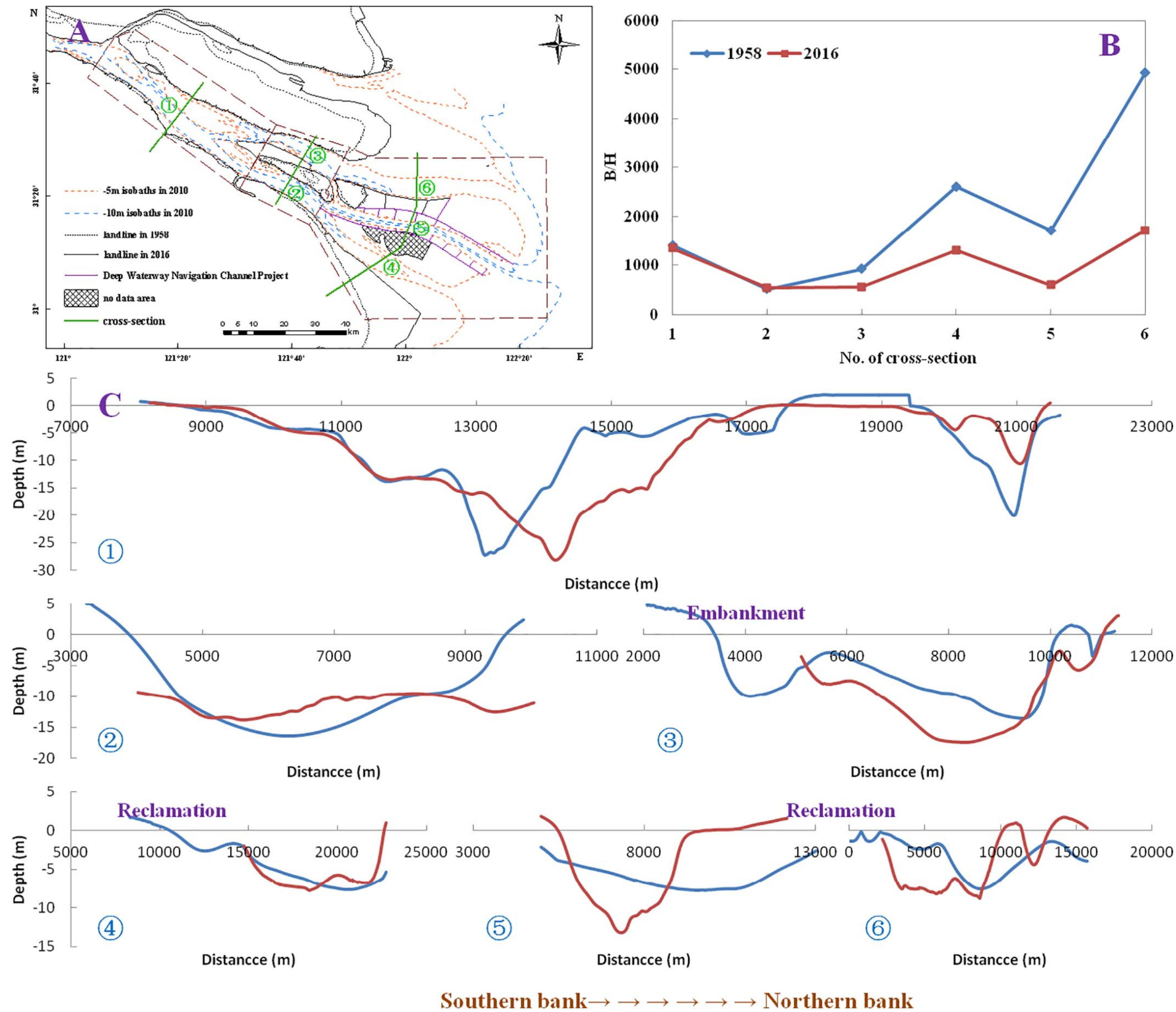

Fig. 6. (A) Location of 6 chosen cross-sections in the Changjiang Estuary. (B) Width to depth ratios of 6 cross-sections based at 0 m referenced to the TLAT in 1958 and 2016. (C) Morphological variations of 6 cross-sectional profiles in both 1958 and 2016.

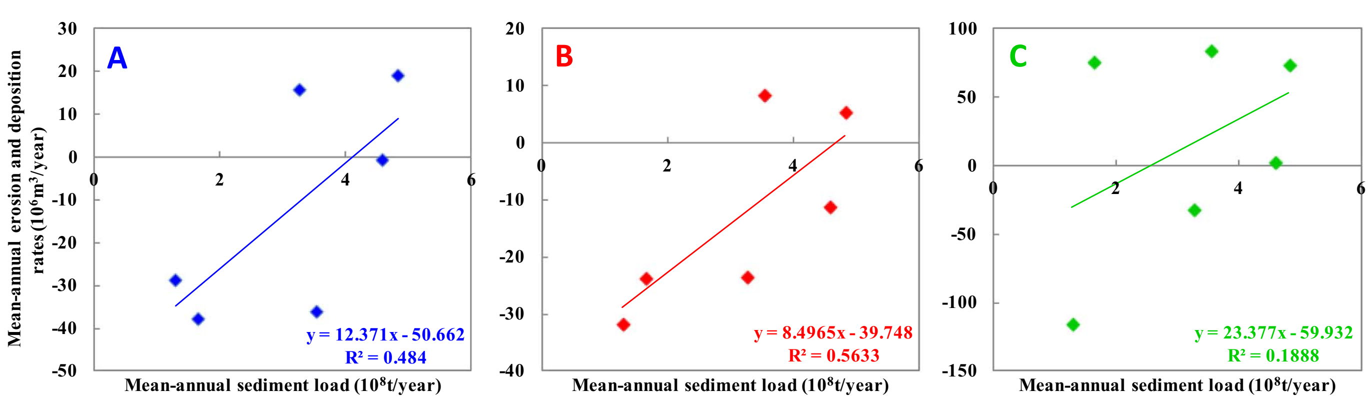

Fig. 7. Comparison of mean annual erosion/deposition rates in region A (A), region B (B), and the MBZ (C) with mean annual sediment load at Datong during the different periods.

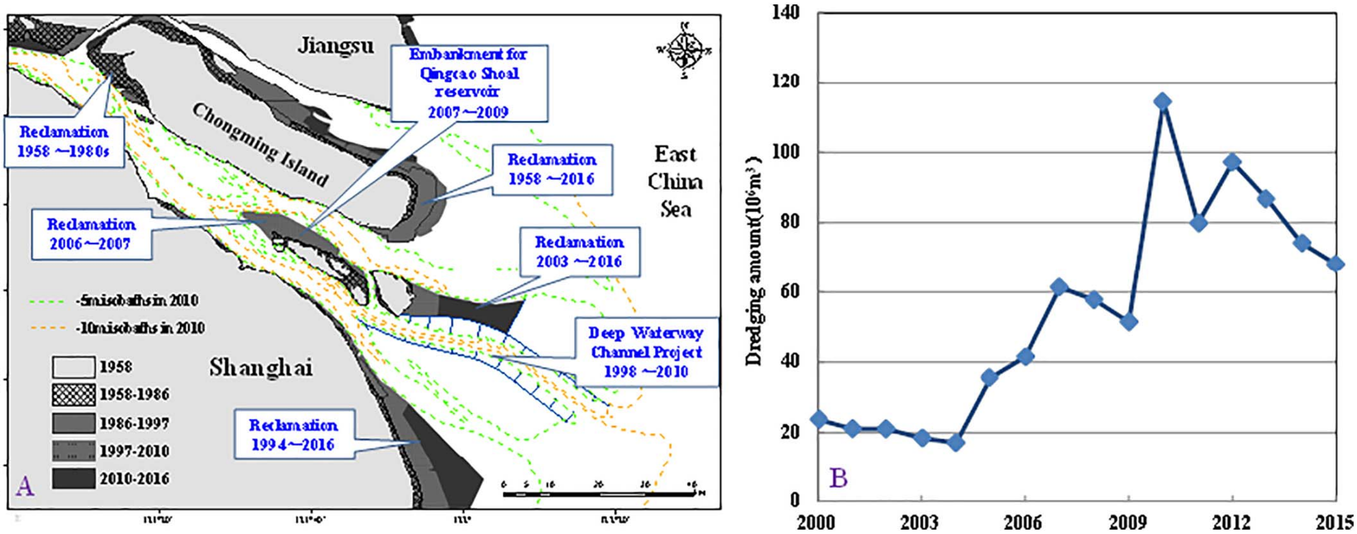

Fig. 8. (A) Change of the shorelines and main large hydraulic constructions in the Changjiang Estuary different periods. (B) Annual dredging amount in the North Passage in the Changjiang Estuary.

the estuary will be more stabilized in the future.

Future work by using morphodynamic modeling is needed to better quantify the time lag and explain the controls of spatial morphological variability.

Acknowledgements

This work is financially supported by the National Natural Science Foundation of China (Nos. 51739005, 51210105005, and 41506105) and the Shanghai Science and Technology Foundation (Nos. 17DZ1204800 and 16DZ1205403). L.C. Guo is also supported by SKLEC-Fund (2015RCDW02) and China Post-doc Fund (2016T90351). The authors thank Prof. Jian Shen, Mr. Lei Zhu, and Mr. Dai Zhang for their internal review and remarks. Constructive comments from reviewers and editors are also thanked.

References

Ahnert, F., 1960. Estuarine meanders in the Chesapeake Bay area. Geogr. Rev. 50 (3), 390–401.
Andrén, H., 1994. Development of the Laitaure delta, Swedish Lapland: a study of growth, distributary forms, and processes. (Ph.D. Dissertation of Uppsala University, Uppsala, Sweden).
Changjiang Water Resources Commission (CWRC), 2015. Changjiang River Sediment Bulletin. Changjiang Press, Wuhan, China (in Chinese).
Chen, J., Li, D., 2002. Regulation of the Changjiang Estuary: past, present and future. In: Engineered Coasts. Springer Netherlands, pp. 185–197.
Chen, J.Y., Zhu, H.F., Dong, Y.F., Sun, J.M., 1985. Development of the Changjiang estuary and its submerged delta. Cont. Shelf Res. 4 (1–2), 47–56.
Chen, J., Li, D., Chen, B., Hu, F., Zhu, H., Liu, C., 1999. The processes of dynamic sedimentation in the Changjiang Estuary. J. Sea Res. 41 (1), 129–140.
Chen, Z., Xu, K., Masataka, W., 2007. Dynamic hydrology and geomorphology of the Yangtze River. In: Gupta, A. (Ed.), Large Rivers: Geomorphology and Management, pp. 457–469.
Chen, X., Yan, Y., Fu, R., Dou, X., Zhang, E., 2008. Sediment transport from the Yangtze River, China, into the sea over the post-three gorge dam period: a discussion. Quat. Int. 186 (1), 55–64.
Chu, Z., Yang, X., Feng, X., Fan, D., Li, Y., Shen, X., et al., 2013. Temporal and spatial changes in coastline movement of the Yangtze delta during 1974-2010. J. Asian Earth Sci. 66, 166–174.
Cowell, P.J., Thom, B.G., 1994. Morphodynamics of coastal evolution. In: Carter, R.W.G., Woodroffe, C.D. (Eds.), Coastal Evolution. Late Quaternary Shoreline Morphodynamics. Cambridge University Press, Cambridge, pp. 33–86.
Dai, Z., Liu, J.T., Wei, W., Chen, J., 2014. Detection of the three gorges dam influence on the Changjiang (Yangtze River) submerged delta. Sci. Rep. 4 (6600), 6600.
De Vriend, H.J., Wang, Z.B., Ysebaert, T., Herman, P.M., Ding, P.X., 2011. Eco-morphological problems in the Yangtze Estuary and the Western Scheldt. Wetlands 31 (6), 1033–1042.
Edmonds, D.A., Slingerland, R.L., 2007. Mechanics of river mouth bar formation: implications for the morphodynamics of delta distributary networks. J. Geophys. Res. Earth Surf. 112 (F2), 237–254.
Freire, P., Taborda, R., Bertin, X., Guerreiro, M., Fortunato, A.B., Silva, A.M., Andrade, C., Oliveira, A., Antunes, C., Freitas, M.C., Nahon, A., Rodrigues, M., Bruneau, N., 2011. Medium-term morphodynamic evolution of a small coastal inlet. J. Coast. Res. 56 (SI 64), 666–670.
Guo, L.C., 2014. Modeling Estuarine Morphodynamics Under Combined River and Tidal Forcing (PH.D. Dissertation of Delft University of Technology). CRC Press.
Guo, L., Wegen, M., Roelvink, J.A., He, Q., 2014. The role of river flow and tidal asymmetry on 1-D estuarine morphodynamics. J. Geophys. Res. Earth Surf. 119 (11), 2315–2334.
Guo, L., Mick, V.D.W., Jay, D.A., Matte, P., Wang, Z.B., Roelvink, D., He, Q., 2015. River-tide dynamics: exploration of nonstationary and nonlinear tidal behavior in the Yangtze River estuary. J. Geophys. Res. Oceans 120 (5), 3499–3521.
He, Q., Guo, L., Liu, H., Wang, Y., 2015. Changjiang Estuary Sediment Transport Dynamics. In: Ecological Continuum from the Changjiang (Yangtze River) Watersheds to the East China Sea Continental Margin. Springer International Publishing, pp. 47–69.
Jiang, C.J., Li, J.F., de Swart, H.E., 2012. Effects of navigational works on morphological changes in the bar area of the Yangtze Estuary. Geomorphology 139, 205–219.
Jiang, C.J., de Swart, H.E., Li, J.F., Liu, G.F., 2013. Mechanisms of along-channel sediment transport in the north passage of the Yangtze Estuary and their response to large-scale interventions. Ocean Dyn. 63 (2–3), 283–305.
Kuang, C., Liu, X., Gu, J., Guo, Y., Huang, S., Liu, S., Yu, W., Huang, J., Sun, B., 2013. Numerical prediction of medium-term tidal flat evolution in the Yangtze Estuary: impacts of the Three Gorges project. Cont. Shelf Res. 52 (1), 12–26.
Liu, H., He, Q., Wang, Z.B., Weltje, G.J., Zhang, J., 2010. Dynamics and spatial variability of near-bottom sediment exchange in the Yangtze Estuary, China. Estuar. Coast. Shelf Sci. 86 (3), 322–330.
Luan, H.L., Ding, P.X., Wang, Z.B., Ge, J.Z., Yang, S.L., 2016. Decadal morphological evolution of the Yangtze Estuary in response to river input changes and estuarine engineering projects. Geomorphology 265, 12–23.
Milliman, J.D., Shen, H.T., Yang, Z.S., Mead, R.H., 1985. Transport and deposition of river sediment in the Changjiang estuary and adjacent continental shelf. Cont. Shelf Res. 4 (1–2), 37–45.
Syvitski, J.P.M., Kettner, A., 2011. Sediment flux and the Anthropocene. Philos. Transact. A Math. Phys. Eng. Sci. 369 (1938), 957.
Syvitski, J.P.M., Kettner, A.J., Correggiari, A., Nelson, B.W., 2005. Distributary channels and their impact on sediment dispersal. Mar. Geol. 222, 75–94.
Toffolon, M., Crosato, A., 2007. Developing macroscale indicators for estuarine morphology: the case of the Scheldt Estuary. J. Coast. Res. 23 (1), 195–212.
Van den Berg, J.H., Jeuken, M.C.J.L., Van der Spek, A.J.F., 1996. Hydraulic processes affecting the morphology and evolution of the Westerschelde estuary. In: Nordstorm, K.F. (Ed.), Estuarine Shores: Evolution. Environments and Human Alterations. John Wiley, London, pp. 157–184.
Van Veen, J., van der Spek, A.J., Stive, M.J., Zitman, T., 2005. Ebb and flood channel systems in the Netherlands tidal waters. J. Coast. Res. 21 (6), 1107–1120.
Wang, Z.B., Ding, P.X., 2012. The branching channel network in the Yangtze Estuary. In: Coastal Engineering Research Council. 1(33).
Wang, Y.H., Ridd, P.V., Wu, H.L., Wu, J.X., Shen, H.T., 2008. Long-term morphodynamic evolution and the equilibrium mechanism of a flood channel in the Yangtze Estuary (China). Geomorphology 99 (1–4), 130–138.
Wang, Y.H., Shen, H.T., LI, J.F., Mao, Z.C., 2011. Geomorphologic features and transport of sandwaves in the flood and ebb channels of the Changjiang Estuary. Oceanol. Limnol. Sin. 42 (2), 330–336.
Wang, Y.H., Dong, P., Oguchi, T., Chen, S.L., Shen, H.T., 2013. Long-term (1842-2006) morphological change and equilibrium state of the Changjiang (Yangtze) Estuary, China. Cont. Shelf Res. 56, 71–81.

Wang, H., Ge, Z., Yuan, L., Zhang, L., 2014. Evaluation of the combined threat from sea-level rise and sedimentation reduction to the coastal wetlands in the Yangtze Estuary, China. Ecol. Eng. 71 (71), 346–354.
Wei, W., Tang, Z., Dai, Z., Lin, Y., Ge, Z., Gao, J., 2015. Variations in tidal flats of the Changjiang (Yangtze) Estuary during 1950s–2010s: future crisis and policy implication. Ocean Coast. Manag. 108, 89–96.
Wright, L.D., 1977. Sediment transport and deposition at river mouths: a synthesis. Geol. Soc. Am. Bull. 88 (6), 857–868.
Wu, J., Wang, Y., Cheng, H., 2009. Bedforms and bed material transport pathways in the Changjiang (Yangtze) Estuary. Geomorphology 104 (3), 175–184.
Wu, H., Zhu, J.R., Choi, B.H., 2010. Links between saltwater intrusion and subtidal circulation in the Changjiang Estuary: a model-guided study. Cont. Shelf Res. 30 (17), 1891–1905.
Wu, J.X., Liu, J.T., Wang, X., 2012. Sediment trapping of turbidity maxima in the Changjiang Estuary. Mar. Geol. 303-306 (1), 14–25.
Yang, S.L., Belkin, I.M., Belkina, A.I., Zhao, Q.Y., Zhu, J., Ding, P.X., 2003. Delta response to decline in sediment supply from the Yangtze River: evidence of the recent four decades and expectations for the next half-century. Estuar. Coast. Shelf Sci. 57 (4), 689–699.
Yang, S.L., Zhang, J., Zhu, J., Smith, J.P., Dai, S.B., Gao, A., Li, P., 2005. Impact of dams on Yangtze River sediment supply to the sea and delta intertidal wetland response. J. Geophys. Res. Earth Surf. 110 (F3), 247–275.
Yang, S.L., Milliman, J.D., Li, P., Xu, K., 2011. 50,000 dams later: erosion of the Yangtze River and its delta. Glob. Planet. Chang. 75 (1), 14–20.
Yin, D.W., Chen, Z.Y., 2009. The Changjiang sediment flux into the seas: measurability and predictability. Front. Earth Sci. China 3 (2), 146–153.
Yun, C.X., 2004. Recent Developments of the Changjiang Estuary. China Ocean Press, Beijing.